



The effect of Clark-Y airfoil vortex generators on tapered NACA 0020 wing Clark-Y uçak kanadı profiline sahip girdap üreteçlerinin konik NACA 0020 kanat üzerindeki etkisi

Mehmet Seyhan^{1,*} , Aleyna Çolak² , Mustafa Sarıoğlu³ 

^{1,2,3} Karadeniz Technical University, Mechanical Engineering Department, 61080, Trabzon, Türkiye

Abstract

In the experimental study, the effects of vortex generators (VGs) having Clark-Y airfoil and triangular VGs were investigated. The aim was to understand how the placement and design of the VGs impact the aerodynamic characteristics of wing. The tests were carried out on a tapered swept-back wing at $Re = 6.0 \times 10^4$ using counter-rotating vortex generators having Clark-Y airfoil at five different locations ($x/c = 0.1, 0.2, 0.3, 0.4,$ and 0.5) and triangular VGs at the $x/c = 0.1$ location. A load cell is used to measure forces at angles of attack (AoA) ranging from 0° to 30° . It is observed that the maximum lift coefficient (C_{Lmax}) and aerodynamic performance of VGs having Clark-Y airfoil decrease when the position of the vortex generators changes from 0.1 to 0.5. The optimal results obtained from the study show that the tapered swept-back wing with the VGs having Clark-Y airfoil exhibits a significant increase of 37.5% in the C_{Lmax} and approximately 55% in the lift to drag ratio (L/D) at $x/c = 0.1$ compared with the baseline. At low AoA, the VGs having Clark-Y airfoil provided better lift, whereas at high AoA, the triangular VGs provided better lift. The drag coefficient of triangular VGs is higher than that of the baseline model and airfoil shaped VGs. This causes airfoil shaped VGs to have higher aerodynamic performance specifically at low AoA. This indicates that VGs having Clark-Y airfoil are effective in improving the aerodynamic performance of the wing.

Keywords: Vortex generators with Clark-Y airfoil, NACA0020, Tapered swept-back wing, Flow control

1 Introduction

Examples of modern applications that operate within the low Reynolds number (Re) regime include micro air vehicles (MAVs) and unmanned aerial vehicles (UAVs) [1], compressor blades [2], and wind turbines [3]. In this flow regime, flows have a higher boundary layer thickness and are more susceptible to flow separation, resulting in reduced aerodynamic performance with decreased lift, increased drag, and aerodynamic noise generation. In the low Re regime, laminar separation is triggered by the existence of a negative pressure gradient. Understanding and strategically modifying boundary layer characteristics offer opportunities

Öz

Bu deneysel çalışmada Clark-Y uçak kanadı şekilli girdap üreteçleri ve üçgensel girdap üreteçlerinin (GÜ) konik geriye ok açılı kanat üzerindeki etkileri incelenmiştir. Bu çalışmanın amacı, GÜ'lerin yerleşimi ve tasarımının kanadın aerodinamik özelliklerini nasıl etkilediğini anlamaktır. Testler, ters dönen aero-şekilli girdap üreteçleri $x/c = 0.1, 0.2, 0.3, 0.4$ ve 0.5 konumlarında, geleneksel girdap üreteçleri $x/c=0.1$ konumunda kullanılarak $Re = 6.0 \times 10^4$ Reynolds sayısında gerçekleştirilmiştir. 0° ila 30° arasında değişen hücum açılarındaki kuvvetleri ölçmek için bir yük hücresi kullanılmıştır. Clark-Y uçak kanadı şekilli GÜ'lerin konumu $x/c=0.1$ 'den 0.5 'e değişmesiyle C_{Lmax} değerinin ve bu değer elde edildiği hücum açılarındaki düşüşü görülmektedir. Çalışmadan elde edilen optimal sonuçlar, Clark-Y uçak kanadı şekilli GÜ'lerin $x/c=0.1$ konumunda, temel modele kıyasla C_{Lmax} değerinde %37.5 ve aerodinamik performansta yaklaşık %55 oranında önemli bir artış sağladığını göstermektedir. Düşük hücum açılarında Clark-Y uçak kanadı şekilli GÜ'ler daha iyi taşıma sağlarken, yüksek hücum açılarında üçgensel GÜ'ler daha iyi taşıma oluşturmuştur. Üçgensel GÜ'lerin sürüklenme katsayısı düz modele ve uçak kanadı şekilli GÜ'lere göre daha yüksektir. Bu da uçak kanat şekilli GÜ'lerin aerodinamik performansının özellikle düşük açılarda daha yüksek olmasına neden olmaktadır. Bu durum Clark-Y kanat profiline sahip GÜ'lerin kanadın aerodinamik performansını artırmada etkili olduğunu göstermektedir.

Anahtar kelimeler: Clark-Y şekilli girdap üreteci, NACA 0020, Konik geriye ok açılı kanat, Akış kontrol

for effective flow control, allowing engineers to prevent or postpone flow separation through targeted interventions. It is possible to add momentum to the boundary layer to delay flow separation by allowing the flow to transition from laminar to turbulent. With more adverse pressure gradients, a turbulent boundary layer may flow with no separation compared to a laminar boundary layer. This is because turbulent mixing increases the transfer of momentum inside the boundary layer. For aerodynamic applications, many flow control methods have been researched and developed. The selection of a suitable flow control method depends on the specific aerodynamic performance goals and the specific application. These can include actively, such as movable

* Sorumlu yazar / Corresponding author, e-posta / e-mail: mehmetseyhan@ktu.edu.tr (M. Seyhan)

Geliş / Recieved: 15.02.2024 Kabul / Accepted: 03.04.2024 Yayınlanma / Published: 15.07.2024

doi: 10.28948/ngumuh.1437429

flaps, blowing or suction, synthetic jet actuators, and passively, such as vortex generators, riblets, and roughness elements on the surface of a wing [4,5].

Vortex generators (VGs) are frequently used flow control devices that manipulate the airfoil around an object, such as a bluff or an aerodynamic body, leading to vortices. Taylor [6] conducted the first experiments on vane-type VGs. The described devices comprise an array of small plates or airfoils placed at an incidence angle relative to the flow to prevent separation in diffuser ducts. Utilizing VGs as a tool for flow control can delay the stall condition, resulting in significantly higher lift characteristics at the critical AoA. The generation of vortices can be used to improve the momentum transfer for all types of VGs. VGs are preferred because they do not have complex parts, are easy to assemble, and are inexpensive. The aerodynamic performance of thick airfoils can be improved by utilizing VGs [7]. Many research investigations have been performed with the aim of fully understanding the working principles behind VGs and enhancing their performance. An effective way of improving efficiency involves using vane-type devices with reduced height to generate streamwise vortices.

Lin [8] provides a comprehensive review of several studies on flow separation control via low profile VGs. They proved that if the height of the standard VGs is reduced below the local boundary layer thickness, momentum transfer remains sufficient to prevent or postpone flow separation. Seshagiri et al. [9] examined the impact of VGs at low Re and showed that static VGs increase the maximum lift coefficient (C_{Lmax}) by 25% and delay the stall angle. Fouatih et al. [10] conducted a study, both experimental and numerical, to examine the influence of triangular VGs. They observed that the L/D of airfoil increases at low AoA with an increase in spanwise separation length; however, it decreases at higher AoA. Another study by Fouatih et al. [11] focused on experimentally optimizing the aerodynamic performance of a NACA 4415 airfoil using VGs to manage flow separation. A comprehensive parametric investigation involving five geometric parameters was conducted, namely height, thickness, position, orientation angle relative to the mean flow, and spanwise spacing of VGs. According to their findings, with regards to the stream-wise location effect, reducing its value from 0.5c to 0.3c results in an increase in

the C_{Lmax} . However, this also increases the drag for rectangular VGs. Fundamentally, the efficiency of VGs is determined by device geometry parameters. Several variables, including the shape, size, and orientation of VGs, may affect flow control. To determine the most efficient arrangement, several studies have focused on the design of VGs under various flow conditions [12-14]. There are two main configurations that are co-rotating and counter-rotating VGs, which differ in their inclination associated with the incoming flow. In the co-rotating arrangement, all VGs have the same angle in relation to the incoming flow. On the other hand, the counter-rotating configuration involves the use of pairs of VGs inclined to the incoming flow but with opposing orientations. The vane type is the most common type of VG and typically involves a small rectangular or triangular plate that is perpendicular to the surface and mounted at an incidence angle in relation to the incoming flow. Furthermore, there are several other types of VGs, such as wishbones [15], doublets, and forward/backward wedges [8]. Numerous investigations have examined unconventional VGs in attempt to identify forms that provide less flow resistance to lower drag. Arunvinthan et al. [16] conducted research to determine the impact of vortex generators based on shark scales (SSVGs) on the aerodynamic characteristics of a symmetrical NACA 0015 profile airfoil. Based on the results of the study, the overall aerodynamic performance was enhanced by SSVGs because they reduced drag and increased C_{Lmax} . Furthermore, Natarajan et al. [17] investigated the impact of utilizing bio-inspired VGs on the hydrodynamic characteristics of a submarine. Both numerical simulations and experimental results indicate that the implementation of shark skin VGs on the lateral side of a submarine can significantly reduce drag in all three degrees of motion: linear, yaw, and pitch movements. Recent research has discovered that denticle VGs can generate lift, leading to a notable rise in the L/D ratio. Earlier investigations regarding the skin of sharks have focused primarily on reducing drag [18]. Considering studies in the literature inspired by shark skin, it has been observed that changing the shape of the VG can increase aerodynamic performance. Thus, improvement can be achieved in different models by using VGs based on airfoil profile, as summarized below.

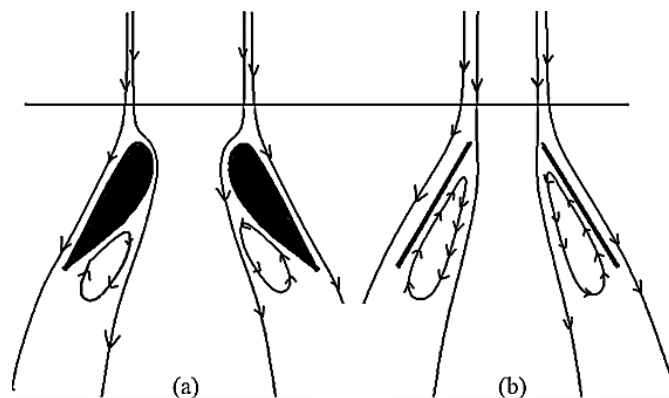


Figure 1. (a) Aerodynamically shaped [19] and (b) conventional VGs [20]

Improvements can be achieved in various models using VGs based on the airfoil profile. Some of these improvements through various studies are summarized below. Hansen et al. [19] proposed VGs with an airfoil shape, as shown in Figure 1(a). They showed that aerodynamically shaped VGs have better L/D compared with standard vane-type VGs. Wang et al. [20] proposed aero-shaped VGs as an alternative to plate-shaped VGs for wind turbine blades. The results showed that aerodynamically shaped VGs provide better aerodynamic performance than standard plate VGs. Moreover, they introduced two configurations of aerodynamically shaped airfoils because of the asymmetric characteristics of Clark-Y airfoil. They demonstrated that the airfoil shaped and triangular VG designs altered the airfoil's aerodynamic performance in Figure 1(a) and were higher than that of the plate VGs in Figure 1(b). Méndez and Gutiérrez [21] compared conventional VGs with rectangular shapes and unconventional VGs with non-symmetrical thin airfoils like Clark-Y and RonCZ. The use of unconventional VGs minimizes the area of flow separation, resulting in reduced drag while simultaneously improving the overall efficiency. Martinez et al. [22] conducted a study on a different kind of VGs known as rod VGs, which was specifically designed to investigate the possibility of aerodynamic enhancement. Rod shape VGs can enhance aerodynamic performance by mitigating flow separation, and the most effective configuration was determined to be at a mid-chord location. Heyes and Smith [23] conducted a detailed analysis of the interaction mechanism between a wing tip with different VGs which are semi-circular, aero-shape based on NACA 0012 airfoil, rectangular, and triangular. They considered triangular VGs to be the best shape among the VGs tested with a lower lift penalty in terms of circulation redistribution. In the study by Algan et al. [24], the impact of aero-shaped VGs on flow around the NACA 4415 airfoil was investigated

and compared with conventional VGs through force and flow visualization experiments at $Re = 1.4 \times 10^5$. Their findings revealed that conventional VGs increased lift coefficient and delayed stall angles; however, they also resulted in an overall increase in drag coefficient. In addition, aero-shaped VGs reduced drag more effectively than conventional VGs, leading to higher L/D.

As mentioned in the above review of the literature, a limited number of studies related to airfoil shaped VGs are available. Therefore, a study related to VGs having an airfoil shape placed on the surface of a tapered swept-back wing was performed to fill the gap in the literature. In this study, the influence of airfoil shaped VGs on a tapered swept-back wing at five chordwise locations was investigated at low Reynolds numbers of 6.0×10^4 . In addition, conventional VGs with the same geometrical parameters as airfoil shaped VGs were created and compared at 10% of the chord location.

2 Material and methods

The aerodynamic characteristics of a tapered swept-back wing was investigated in the suction type wind tunnel. There was less than 1% turbulence in the test section of this tunnel, which is 57 cm by 57 cm in square. The frequency inverter was used to adjust the free-stream velocity. Figure 2(a and b) shows a schematic view of the measurement system, which consists of a rotary unit, a 6-axis ATI Gamma DAQ F/T load cell, a connection rod, a test model, a protection pipe, and end plates.

As shown in Figure 2(b), the test model is mounted vertically to the load cell system with a connection rod. To provide a proper AoAs, load cell is mounted on a rotating mechanism. The end plate is attached to the lower wall, and there is never more than a 2 mm space between it and the test model.

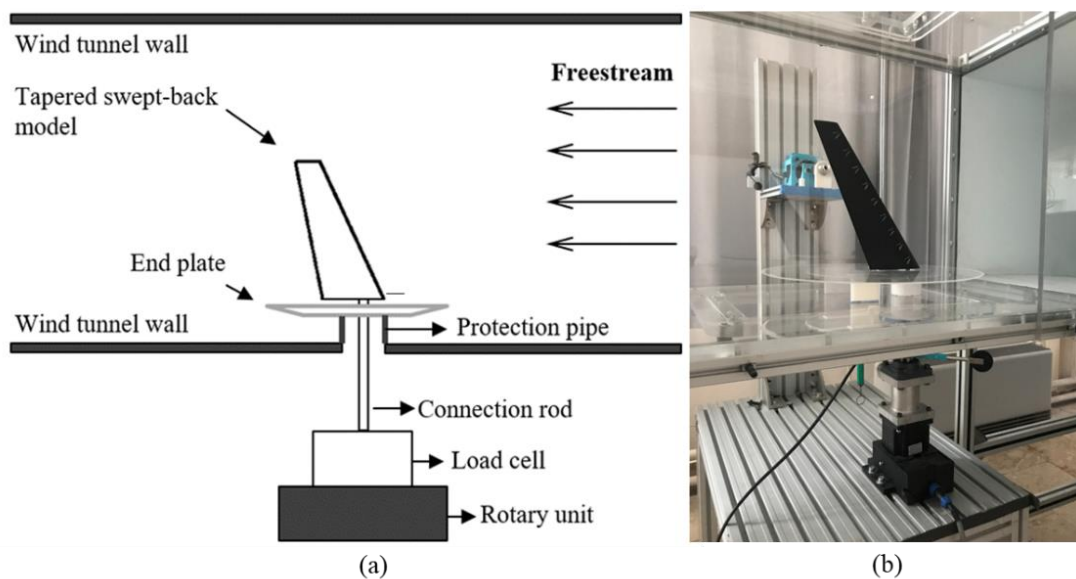


Figure 2. (a) Schematic view of the force measurement system and (b) NACA 0020 airfoil with VGs in the wind tunnel

Experiments were carried out at AoAs between 0° and 30°. Force measurements were taken as 20000 samples for 10 seconds. The experiments were performed at a mean chord-based Re of 6.0×10^4 . The test model was created from PLA material using a 3D printer from CCH Technology, model MY Z35, and sanded from coarse to fine to obtain a smooth surface. The choice of taper was made because sweeping wings frequently have a taper to reduce induced drag. The test model has a mean aerodynamic chord (c) of 89 mm and a NACA 0020 airfoil section. The geometric parameters of the test model are 120 mm for the root chord, 48 mm for the tip chord, and 270 mm for the span. The model has a taper ratio of 0.4 and a sweep angle of 35°. The dimensions were selected with consideration for blockage effects, and the blockage ratio (BR) at the highest AoA was maintained below 6%. According to Choi and Kwon [25], the aerodynamic behavior of bluff bodies showed minimal variation at BR of up to 10%. Katz and Walters [26] advised avoiding cases in which the BR is greater than 7%. In this study, because the BR was within an acceptable range, blockage correction was not performed.

The reliability and validity of the experimental results are enhanced by understanding the limitations and uncertainties related to the instruments used for measurement. The load cell is capable of measuring F_x and F_y within a range of $\pm 32N$, and F_z within a range of $\pm 100N$. The test model and the load cell are aligned parallel to the flow direction using a laser and the AoA measurement has an estimated uncertainty of $\pm 0.2^\circ$ [27].

The lift (C_L) and drag (C_D) coefficients are given as in Equation (1) and (2), respectively, where F_L is the lift force, F_D is the drag force, ρ is the air density (1.19 kg/m^3), U_∞ is the free-stream velocity (10.4 m/s), and A is the planform area of the wing (0.02 m^2). The Reynolds number is a dimensionless quantity used in fluid dynamics to describe the relative importance of inertial forces to viscous forces in a flow, which is represented in Equation (3). The Reynolds number of 6.0×10^4 selected as it falls within the range of the critical Reynolds number stated in the literature [28-29].

$$C_L = \frac{F_L}{0.5\rho AU_\infty^2} \quad (1)$$

$$C_D = \frac{F_D}{0.5\rho AU_\infty^2} \quad (2)$$

$$Re = \frac{\rho * U_\infty * c}{\mu} \quad (3)$$

Godard and Stanislas [30] examined the effect of different VG configurations and types. The results revealed that among various shapes, triangular counter-rotating VGs proved to be the most efficient. Based on this result, conventional VGs were designed as a triangular shape. Conventional VGs are made of a metal sheet with a thickness of 0.25 mm. The VGs were placed on a test model with a small piece of double-sided tape. Clark-Y airfoil profile was chosen for the design of VGs. The pressure side of the Clark-Y airfoil makes estimating AoA easier, and its good performance at low Reynolds numbers is the reason for this selection [19]. Clark-Y airfoil shaped VGs are designed in accordance with the delta shape of conventional VGs. The geometric parameters of the triangular and Clark-Y airfoil shaped VGs for the counter-rotating configuration are shown in Figure 3. A pair of VGs has a leading-edge spacing (s) of 5 mm. The dimensions of VGs are 5 mm height (h) and 15 mm length (l). The indicating angle (β) of VG is 13°. The spacing between two pairs of VGs (z) is 35 mm. Clark-Y airfoil shaped VGs were produced using Anycubic Photon Mono-X. The configuration of the airfoil suggested by Wang et al. [20] was considered.

The process of determining system uncertainty involves considering various factors, such as the uncertainties associated with the force measurement system, rotary unit and the data collection card. The measured lift and drag coefficients were estimated to have uncertainties of 3.16% and 3.45%, respectively, utilizing the methodology outlined in Coleman and Steele [31].

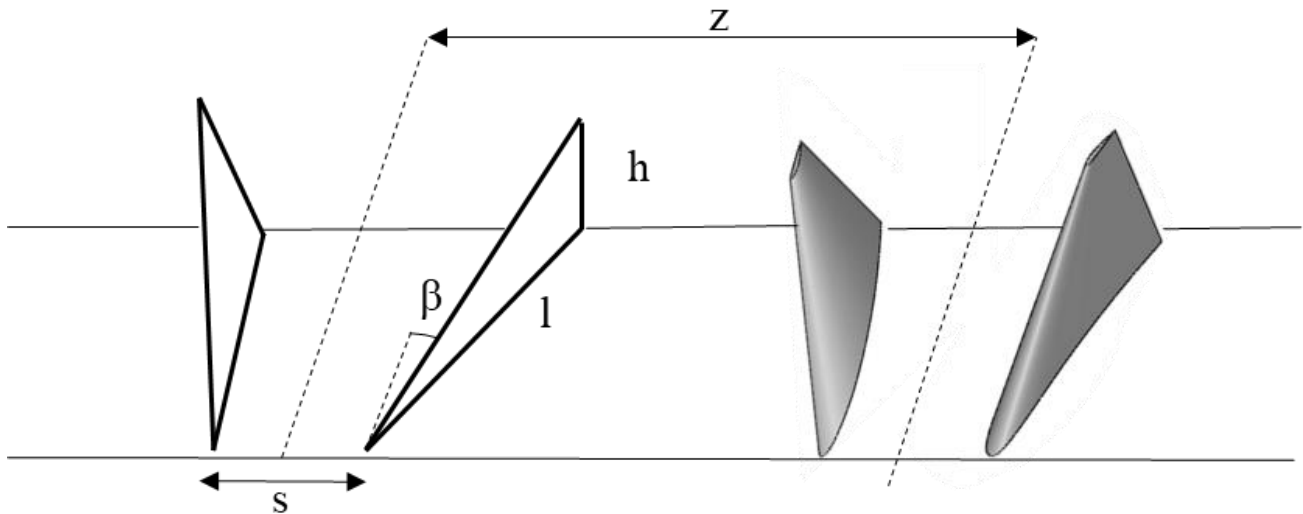


Figure 3. The geometric parameters of airfoil shaped and triangular VGs

Five positions to be tested were chosen as the distances of 10%, 20%, 30%, 40% and 50% of the chord distances from the leading edge (LE). In addition, the aerodynamic characteristics of counter-rotating aero-shape and conventional VGs were compared at 10% of the chord locations. To achieve this, the same geometric parameters were chosen. VGs having airfoil shape are referred to as AVGs, and triangular VGs are referred to as TVGs to avoid confusion. Throughout this article, the term “Baseline” refers to a clean wing without VGs.

3 Results and discussion

In the wind tunnel, the F_L and F_D acting on the tapered swept-back wing with triangular and Clark-Y airfoil-shaped VGs were measured to determine the impact of VGs location (x/c). The comparison of lift coefficients of tapered swept-back wing with AVGs is plotted for various chord positions that are $x/c = 0.1, 0.2, 0.3, 0.4,$ and 0.5 in Figure 4(a). The baseline model did not experience a stall phenomenon and demonstrated a continuous increase in lift. Up to 10° , all configurations with VGs have a C_L higher than the baseline. The lift coefficient of the AVGs at $x/c = 0.1$ and $x/c = 0.2$ showed better performance than that of the baseline up to 24° , especially at lower AoA. AVGs mounted at $x/c = 0.1$ provided a 37.5% improvement in lift at an AoA of 15° . However, the AVGs mounted at $x/c = 0.2$ provided a 27.5% augment in lift at the AoA of 13° . Vortex generators positioned at $x/c = 0.1$ demonstrate a higher lift coefficient within the AoA range of 17° to 24° compared with vortex generators mounted at $x/c = 0.2$. AVGs produced more C_L at the location of $x/c = 0.1$ than $x/c = 0.2$ at AoAs between 11° and 23° . After 23° , no improvement was observed at the positions of $x/c = 0.3, x/c = 0.4$ and $x/c = 0.5$. As the AoA increases, there is a trend where, as the position approaches

the trailing edge, both the lift obtained and the AoA decrease. Specifically, at position 0.1, C_{Lmax} was achieved at 15° . In contrast, at positions 0.2, 0.3, and 0.4, C_{Lmax} values were attained at AoAs of $12^\circ, 7^\circ,$ and 6° , respectively. Notably, the position 0.5 exhibits an increasing lift curve like that of the baseline model.

These results indicate that the position of the VGs along the chord has an important impact on the C_L . It is observed that the increase in the location of the VGs between $x/c = 0.1$ and $x/c = 0.5$ causes a reduction in C_{Lmax} and corresponding maximum AoA. The reason for this phenomenon is the displacement of VGs toward the trailing edge (TE) of the wings. When VGs are placed nearer to the wing’s leading edge (LE), they have a greater ability to manipulate the flow and prevent it from separating from the surface of wing. However, as the VGs move toward the TE, the separated flow remains within the wake region of the wing, reducing the effectiveness of the VGs. As a result, to achieve a higher C_L , the vortex generators should be located at a lower position along the chord. These results are compatible with the results of Fouatih et al. [10]. They showed that for a smaller value of location, a higher C_L may be attained with TVGs.

Another study by Fouatih et al. [11] highlighted improvements in the aerodynamic performance of the maximum lift coefficient for $x/c = 0.3c, 0.4c,$ and $0.5c$, reporting enhancements of 10.6%, 11.3%, and 7.8%, respectively. The study elucidated the influence of stream-wise location, indicating that higher lift coefficients can be achieved when the VGs are placed in closer proximity to the LE, corresponding to lower values along the chord. The results of the literature highlight the connection between aerodynamic performance and VG location, offering insightful information for improving wing design.

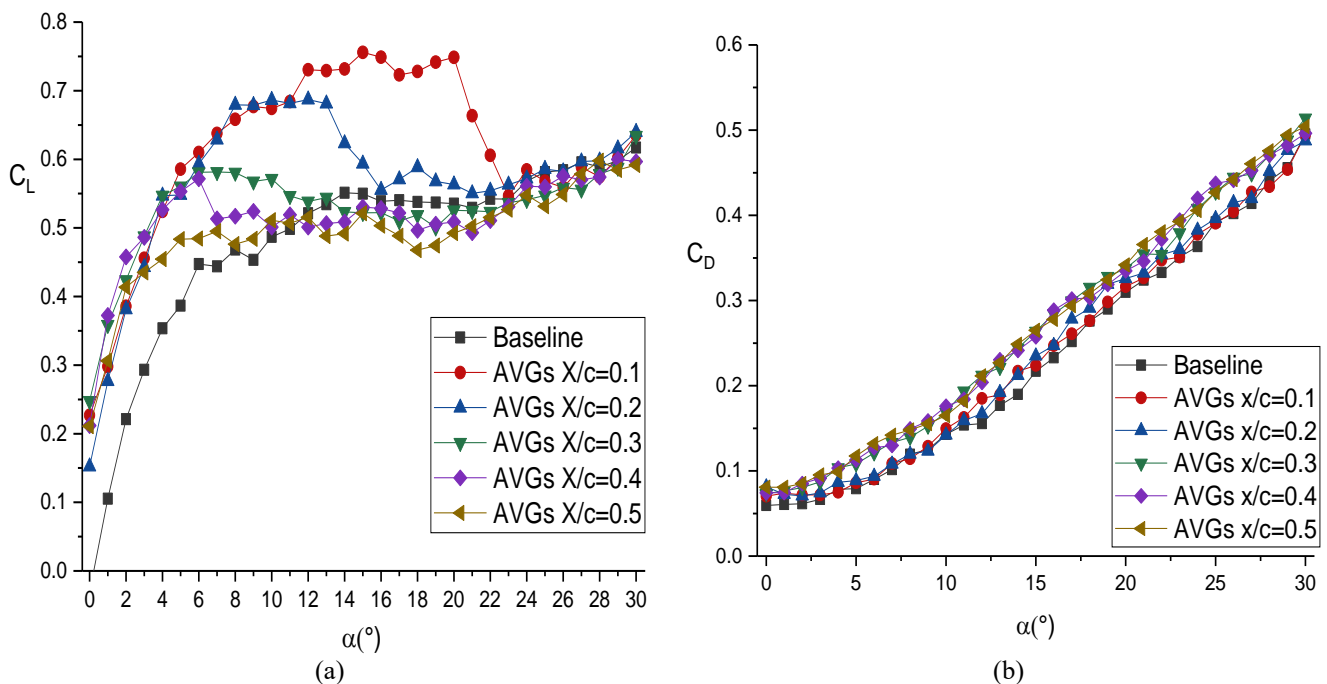


Figure 4. Changes in the (a) C_L and (b) C_D with respect to AoA at $x/c = 0.1, 0.2, 0.3, 0.4,$ and 0.5

The drag characteristics of the AVGs at different chord locations are shown in Figure 4(b). For AVGs at $x/c = 0.1$ and 0.2 , the drag coefficients are like the baseline, except for $10^\circ < \alpha < 18^\circ$ and $10^\circ < \alpha < 25^\circ$, respectively. In these ranges, AVGs for both locations have a higher drag coefficient than baseline. For the positions of $x/c = 0.3, 0.4,$ and 0.5 , C_D is greater than the baseline for the entire AoAs. These findings suggest that the position of AVGs along the chord of an airfoil affects its aerodynamic characteristics [10]. The C_D at $x/c = 0.3, 0.4,$ and 0.5 exhibit higher values than those at positions $x/c = 0.1$ and 0.2 .

Figure 5 presents the L/D (C_L/C_D) ratios with respect to the AoAs for $x/c = 0.1, 0.2, 0.3, 0.4$ and 0.5 various locations at $Re=6.0 \times 10^4$. Both L/D and C_L/C_D ratios are indicators of aerodynamic efficiency. Although there was no reduction in drag, the improvement in lift at higher AoAs resulted in the AVGs at $x/c = 0.1$ and $x/c = 0.2$ positions having better aerodynamic performance at AoAs between 15° and 20° compared to the baseline. AVGs mounted at $x/c = 0.1$ improve the L/D ratio by 55% at 4° . It is seen that AVGs at $x/c = 0.1$ have better aerodynamic performance than those at $x/c = 0.2$ for the majority of the AoA. Up to 4° , the positions of $x/c = 0.3, 0.4,$ and 0.5 have aerodynamic performance like the baseline, but they have lower performance than the baseline at higher angles. Especially at low AoAs, an improvement in L/D is observed at all chord positions. For AVGs mounted at a location of $x/c = 0.2$, a significant improvement of 27.4% in L/D ratio was observed at an AoA of 6° . Surface oil flow visualization results by Seshagiri et al. [32] presents that the VGs divide the bubble into segments for certain VG configurations and reduce the size of the laminar separation bubble. This suggests that the use of VGs is a strategy to achieve a more effective lift at a given AoA.

Flow separation can affect the overall aerodynamic performance by decreasing lift and increasing drag. Algan et al. [24] suggested that at $x/c = 0.1$, the aero-shaped model provides a larger reattached area on the surface of the airfoil behind the VG pairs, termed the reattached flow region, compared to conventional VGs. This difference in attached flow region can impact the aerodynamic performance of the airfoil. The surface oil flow visualization's findings presented that when the VG position changes from $x/c = 0.1$ to $x/c = 0.5$, the VG effect decreases.

Force measurement results showed that while there is no notable alteration in lift at higher AoAs, there is an increase in drag. In addition, placing vortex generators close to TE increase the drag, as shown in Figure 4(b). The higher drag, particularly when vortex generators are closer to the trailing edge, contributes to a decrease in the maximum L/D ratio across chord positions ranging from 0.1 to 0.5 . The observed decrease in the maximum L/D ratio as the chord position of the VGs changes could be attributed to several factors. When VGs are strategically placed near the leading edge, they manage control over the airflow from the initial stages and postpone the onset of separation. This positioning near the leading edge ensures early intervention in the aerodynamic process, delaying any adverse effects associated with flow separation.

The aerodynamic characteristics of AVGs and TVGs with the same parameters at $x/c = 0.1$ for a Reynolds number of 6.0×10^4 are seen in Figure 6(a, b, and c). The best aerodynamic performance performed using AVGs between chord positions is at $x/c = 0.1$. As the position of VGs moves from LE to TE, the C_{Lmax} and aerodynamic performance decrease.

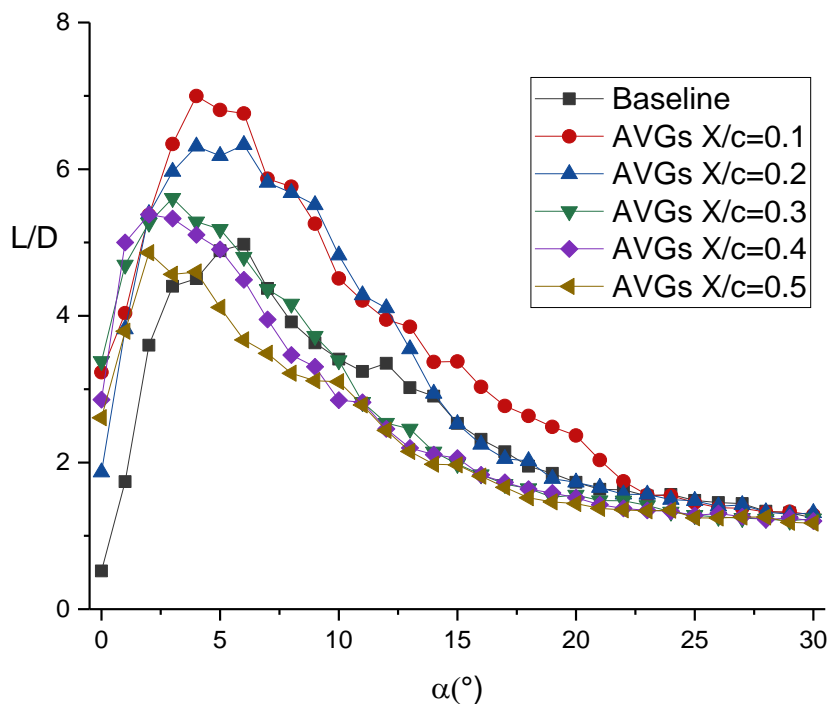


Figure 5. Changes in the L/D with respect to AoA for at $x/c = 0.1, 0.2, 0.3, 0.4,$ and 0.5

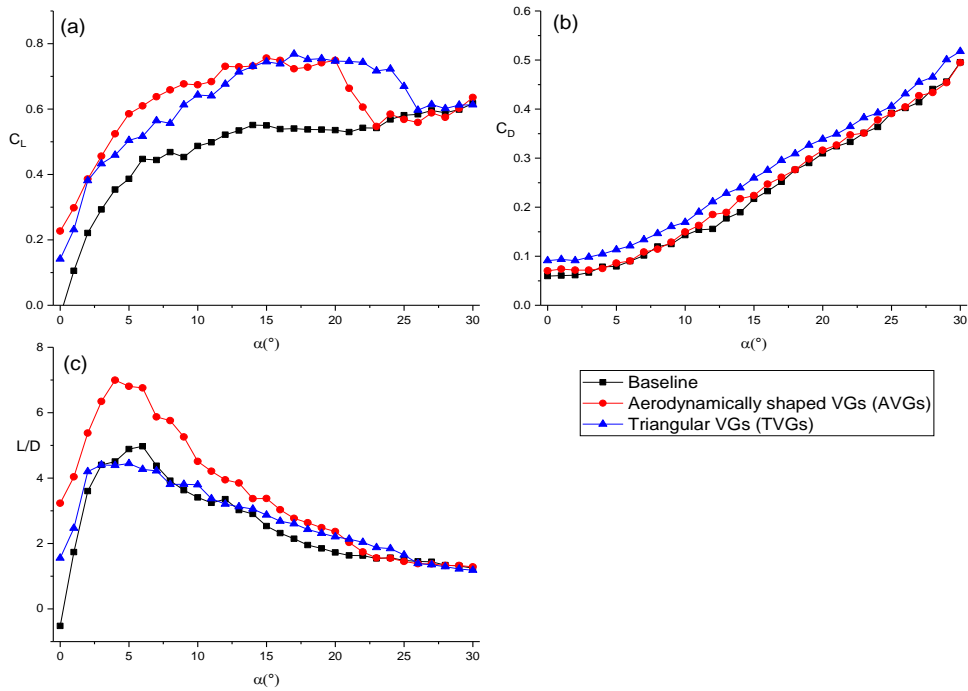


Figure 6. Changes in (a) C_L , (b) C_D , and (c) L/D with respect to AoA at $x/c = 0.1$

To investigate the influence of the shape of the VGs, a comparison of the AVGs and TVGs was performed at the $x/c = 0.1$. In Figure 6 (a and b), C_L and C_D of AVGs and TVGs at $x/c = 0.1$ are compared at AoAs between 0° and 30° . Up to 23° , AVGs and TVGs had a higher C_L than the baseline. At the AoAs between 0° and 17° , AVGs have a higher C_L than TVGs. The TVGs provided a higher lift coefficient than AVGs for the AoAs $20^\circ < \alpha < 30^\circ$. The C_{Lmax} of the AVGs occurs at an AoAs of 15° and is 0.756. The TVGs exhibited a lift coefficient of 0.768 at 17° , indicating an approximately 42% increase in lift coefficient compared with baseline. While providing an improvement in lift, the TVGs have a higher C_D compared to the baseline and the AVGs for the entire measured AoA range.

The flow over conventional VGs typically experiences separation at the leading edge, resulting in significant drag. In contrast, AVGs based on airfoil shape are expected to

exhibit smaller separation, particularly at the leading edge, resulting in decreased drag compared to conventional VGs. AVGs have a similar curve to baseline, except for $9^\circ < \alpha < 23^\circ$. As shown in Figure 6(c), TVGs have a higher performance at higher AoA, whereas AVGs have a higher performance except for the higher AoA. AVGs have better aerodynamic performance than TVGs. In agreement with the literature, VGs having airfoil shape provide better aerodynamic performance (L/D ratio) than conventional vane-type VGs [19-21].

The percentage change in lift and drag performance for AVGs and TVGs as a function of AoAs ranging from 10° to 25° is shown in Figure 7(a and b). TVGs have better lift performance than the AVGs at almost all AoAs considered except for $\alpha = 23^\circ-25^\circ$. However, when considering drag percentage ($\%C_D$), TVGs demonstrate higher drag than AVGs.

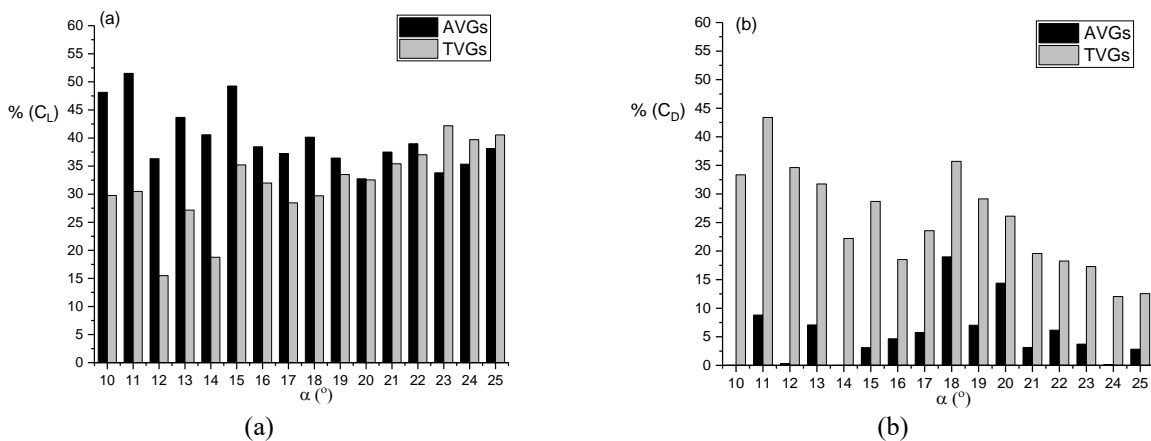


Figure 7. Percentage of AVGs and TVGs versus the baseline model (a) $\%C_L$ and (b) $\%C_D$

4 Conclusions

The influence of chord positions that are $x/c = 0.1, 0.2, 0.3, 0.4,$ and 0.5 is investigated for AVGs on the tapered swept-back wing at Re of 6.0×10^4 . Moreover, considering the same VGs geometric parameters, TVGs and AVGs are compared. VGs having the shape of an airfoil were designed and used to minimize drag and disturbance to the airflow while generating strong vortices that can help delay flow separation and improve L/D ratio. The findings demonstrated that the VGs on the wing increase the C_L . The maximum improvement in C_L belongs to the $x/c = 0.1$ chord location at approximately 37.5% at an AoA of 15° for the AVGs. C_{Lmax} and aerodynamic performance of AVGs decrease as the position of the VGs changes from 0.1 to 0.5. TVGs having a rectangular shape can be simpler to manufacture and install compared with a streamlined airfoil shape, however, they may also introduce more drag compared to an airfoil shape. It was found that AVGs were more effective at improving aerodynamic performance compared to TVGs.

The optimal shape of a VGs with a tapered swept-back wing depends on several factors. These factors can include the desired aerodynamic performance goals, the specific geometric characteristics of the wing, and the operating conditions of the aircraft. In this study, the best configuration is counter-rotating AVGs and a location $x/c=0.1$ streamwise along the chord at low Re condition. The effectiveness of VGs is dependent upon numerous factors, including their shape, dimensions, angle concerning the mean flow direction, leading-edge spacing, and the separation distance between consecutive pairs. To obtain a comprehensive performance of VGs, additional parametric experimentation can be undertaken.

Conflict of interest

The authors declare no conflict of interest.

Similarity rate (iThenticate): 12 %

References

- [1] J. Winslow, H. Otsuka, B. Govindarajan, and I. Chopra, Basic understanding of airfoil characteristics at low Reynolds numbers (10^4 – 10^5), *Journal of aircraft*, 55(3), 1050–1061, 2018. <https://doi.org/10.2514/1.C034415>.
- [2] Q. Liu, W. Ager, C. Hall, and A. P. S. Wheeler, Low Reynolds Number Effects on the Separation and Wake of a Compressor Blade, *Journal of Turbomachinery*, 144(10), 101008, 2022. <https://doi.org/10.1115/1.4054148>.
- [3] Zhao, Z., Jiang, R., Feng, J., Liu, H., Wang, T., Shen, W., and Liu, Y. Researches on vortex generators applied to wind turbines: A review, *Ocean Engineering*, 253, 111266, 2022. <https://doi.org/10.1016/j.oceaneng.2022.111266>.
- [4] M. Gad-el-Hak, Flow control: The future”, *Journal of aircraft*, 38(3), 402–418, 2001. <https://doi.org/10.2514/2.2796>.
- [5] T. Moghaddam and N. B. Neishabouri, On the Active and Passive Flow Separation Control Techniques over Airfoils, *IOP Conference Series: Materials Science and Engineering*, 248, 1, 2017. <https://doi.org/10.1088/1757-899X/248/1/012009>.
- [6] H. D. Taylor, The elimination of diffuser separation by vortex generators, *Res. Dep. Rep. r-4012-3*, United Aircraft Corporation. East Hartford, Connecticut, 103, 1947.
- [7] K. Yang, L. Zhang, and J. Xu, Simulation of aerodynamic performance affected by vortex generators on blunt trailing-edge airfoils, *Science in China Technological Sciences*, 53(1), 1–7, 2010. <https://doi.org/10.1007/s11431-009-0425-5>.
- [8] J. C. Lin, Review of research on low-profile vortex generators to control boundary-layer separation, 38, 4–5, 2002. [https://doi.org/10.1016/S0376-0421\(02\)00010-6](https://doi.org/10.1016/S0376-0421(02)00010-6).
- [9] A. Seshagiri, E. Cooper, and L. W. Traub, Effects of vortex generators on an airfoil at low reynolds numbers, *Journal of aircraft*, 46(1), 116–122, 2009. <https://doi.org/10.2514/1.36241>.
- [10] O. M. Fouatih, B. Imine, and M. Medale, Numerical/experimental investigations on reducing drag penalty of passive vortex generators on a NACA 4415 airfoil, *Wind Energy*, 22(7), 1003–1017, 2019. <https://doi.org/10.1002/we.2330>.
- [11] O. M. Fouatih, M. Medale, O. Imine, and B. Imine, Design optimization of the aerodynamic passive flow control on NACA 4415 airfoil using vortex generators, *European Journal of Mechanics-B/Fluids*, 56, 82–96, 2016. <https://doi.org/10.1016/j.euromechflu.2015.11.006>.
- [12] M. B. Bragg and G. M. Gregorek, Experimental study of airfoil performance with vortex generators, *Journal of aircraft*, 24(5), 305–309, 1987. <https://doi.org/10.2514/3.45445>.
- [13] X. Li, K. Yang, and X. Wang, Experimental and numerical analysis of the effect of vortex generator height on vortex characteristics and airfoil aerodynamic performance, *Energies*, 12(5), 2019. <https://doi.org/10.3390/en12050959>.
- [14] X. kai Li, W. Liu, T. jun Zhang, P. ming Wang, and X. dong Wang, Analysis of the effect of vortex generator spacing on boundary layer flow separation control, *Applied Sciences*, 9(24), 2019. <https://doi.org/10.3390/app9245495>.
- [15] A. Cheawchan, M. A. Mohamed, B. F. Ng, and T. H. New, Flow Structures of Wishbone Vortex Generators and Their Interactions with a Backward-Facing Ramp, *Journal of Aerospace Engineering*, 36(1), 4022120, 2023. <https://doi.org/10.1061/JAEEZ.ASENG-4537>.
- [16] S. Arunvinthan, V. S. Raatan, S. Nadaraja Pillai, A. A. Pasha, M. M. Rahman, and K. A. Juhany, Aerodynamic characteristics of shark scale-based vortex generators upon symmetrical airfoil, *Energies*, 14(7), 2021, <https://doi.org/10.3390/en14071808>.

- [17] E. Natarajan, L. Inácio Freitas, G. Rui Chang, A. Abdulaziz Majeed Al-Talib, C. S. Hassan, and S. Ramesh, The hydrodynamic behaviour of biologically inspired bristled shark skin vortex generator in submarine, *Materials Today: Proceedings*, 46, 83945–3950, 2021. <https://doi.org/10.1016/j.matpr.2021.02.471>.
- [18] A. G. Domel, M. Saadat, J. C. Weaver, H. Haj-Hariri, K. Bertoldi, and G. V. Lauder, Shark skin-inspired designs that improve aerodynamic performance, *Journal of Royal Society Interface*, 15(139), 1–9, 2018. <https://doi.org/10.1098/rsif.2017.0828>.
- [19] M. O. L. Hansen vd., Aerodynamically shaped vortex generators, *Wind Energy*, 19(3), 563–567, 2016. <https://doi.org/10.1002/we.1842>.
- [20] Q. Wang, S. Yang, H. Wang, ve J. Wang, Aerodynamic shape integrated design of wind turbine airfoils and vortex generators, *International Journal of Green Energy*, 19(7), 747–756, 2022. <https://doi.org/10.1080/15435075.2021.1961261>.
- [21] B. Méndez and R. Gutiérrez, Non-conventional vortex generators calculated with CFD, *Journal of Physics: Conference Series*, 1037(2), 2018, <https://doi.org/10.1088/1742-6596/1037/2/022029>.
- [22] J. Martinez Suarez, P. Flaszynski, and P. Doerffer, Streamwise vortex generator for separation reduction on wind turbine profile, *Journal of Physics: Conference Series*, 760(1), 2016. <https://doi.org/10.1088/1742-6596/760/1/012018>.
- [23] A. L. Heyes and D. A. R. Smith, Modification of a wing tip vortex by vortex generators, *Aerospace science and Technology*, 9(6), 469–475, 2005. <https://doi.org/10.1016/j.ast.2005.04.003>.
- [24] M. Algan, M. Seyhan, and M. Sarıoğlu, Effect of aero-shaped vortex generators on NACA 4415 airfoil, 291, 116482, 2024. <https://doi.org/10.1016/j.oceaneng.2023.116482>.
- [25] C. K. Choi and D. K. Kwon, Wind tunnel blockage effects on aerodynamic behavior of bluff body, *Wind and Structures*, 1(4), 351–364, 1998. <https://doi.org/10.12989/was.1998.1.4.351>.
- [26] J. Katz and R. Walters, Investigation of Wind-Tunnel Wall Effects in High Blockage Testing, *AIAA Pap.*, 95–0438, 1995.
- [27] M. Seyhan, M. Sarıoğlu, and Y. E. Akansu, Influence of leading-edge tubercle with amplitude modulation on NACA 0015 airfoil. *AIAA Journal*, 59(10), 3965-3978, 2021. <https://doi.org/10.2514/1.J060180>
- [28] B. Carmichael, Low Reynolds number airfoil survey, NASA-CR-165803- VOL-1 (NASA Lab, 1981).
- [29] P. Lissaman, Low-Reynolds-number airfoils, *Annu. Rev. Fluid Mech.* 15, 223–239, 1983. <https://doi.org/10.1146/annurev.fl.15.010183.001255>
- [30] G. Godard and M. Stanislas, Control of a decelerating boundary layer. Part 1: Optimization of passive vortex generators, *Aerospace Science and Technology*, 10(3), 181–191, 2006. <https://doi.org/10.1016/j.ast.2005.11.007>.
- [31] Hugh W. Coleman and W. Glenn Steele, Experimentation, validation, and uncertainty analysis for engineers, John Wiley & Sons, 1989.
- [32] Seshagiri, Amith, Evan Cooper, and Lance W. Traub. Effects of vortex generators on an airfoil at low Reynolds numbers. *Journal of Aircraft* 46(1), 116-122, 2009. <https://doi.org/10.2514/1.36241>.

